UNIVERSITY OF GOTHENBURG

SAHLGRENSKA ACADEMY

DEVELOPMENT, VALIDATION AND APPLICATION OF A METHOD FOR DETERMINATION OF METABOLITE CONCENTRATIONS WITH PRECLINICAL MAGNETIC RESONANCE SPECTROSCOPY

Lukas Lundholm

Essay/Thesis:	30 hp
Program and/or course:	Medical Physics
Level:	Second Cycle
Semester/year:	Spring 2018
Supervisor:	Mikael Montelius and Oscar Jalnefjord
Examiner:	Magnus Båth

Abstract

Essay/Thesis:	30 hp
Program:	Medical Physics
Level:	Second Cycle
Semester/year:	Spring 2018
Supervisor:	Mikael Montelius and Oscar Jalnefjord
Examiner:	Magnus Båth
Keywords:	MRS, Basis sets, Metabolites, Quantification, Animal study

---

Background: Information on the metabolic content in tissue has diagnostic and prognostic value when examining for example cancer and diseases of the brain. MR spectroscopy is a non-invasive method that allows quantification of metabolite concentrations *in vivo*, without the use of ionizing radiation, which makes the method highly attractive for both research and clinical applications.

However, specialized software is required for generation of so called basis sets, which consist of information on the individual metabolites that are under investigation, and which are required for quantification. Furthermore, method- and MR vendor-specific information must be provided as the basis sets are being generated in order to yield reliable quantification results.

A software for generation of basis sets was recently developed at the University of Gothenburg and validated for a preclinical MR system in a previous master thesis project. However, a standardized method for calculation of metabolite concentrations *in vivo* in the preclinical setting has not yet been developed.

Therefore, the purpose of this work was to adapt, validate and apply a method for non-invasive quantification of metabolites from *in vivo* MR spectroscopy at the preclinical facility at the University of Gothenburg.

Method: The software, implemented in MATLAB and previously developed to simulate basis sets for the clinical MR system, was programmatically adapted to import pulse sequence parameters from the preclinical MR system. Validation of the adapted MATLAB software was done by MR spectroscopy measurements on a phantom solution with known concentrations of certain metabolites, followed by metabolite quantification using the LCModel software. Two *in vivo* experiments were performed to assess the applicability of the method in the preclinical setting: one on the healthy mouse brain and one on a mouse model of human cancer. The point resolved spectroscopy (PRESS) pulse sequence was used for all measurements and simulations.

Results: The adaption of the software to the preclinical MR system was successful, resulting in simulated basis sets that could be well fitted to the spectra measured in the validation which, in turn, resulted in accurate determination of metabolite concentrations in the phantom. The *in vivo* experiments resulted in metabolic profiles of the cancer model and the healthy mouse brain that were in agreement with what has been found in previous studies. The method developed in this work will thus enable metabolite quantification of existing and future MR spectroscopy studies at the preclinical MR facility at the University of Gothenburg.

Table of content

1 Introduction

For a cell to grow, divide and perform its functions it requires energy. The process of converting nutrients to energy and biomass is called metabolism and, involved in this process, are intermediates and products of the metabolism called metabolites (Sand & Toverud, 2007).

In cancer tissue, altered metabolism is required to provide for the rapid cell proliferation and adaption to the hostile microenvironment including, *e.g.*, hypoxia. Thus, the metabolic content inside a tumour differs from that of healthy tissue, and knowledge of the tumour metabolic profile may provide important information on tumour aggressiveness, facilitate diagnosis and enable personalized treatment (Bokacheva et al., 2014).

Magnetic resonance spectroscopy (MRS) is the only non-invasive method with the potential to provide *in vivo* assessment of tissue metabolism without the use of ionizing radiation. MRS is thus highly interesting for diagnosis and for prediction and assessment of tumour therapy response, both in cancer research and in the clinical setting (Gonzalez Hernando et al., 2010). MRS for quantitative assessment of cell metabolism has shown great potential as a tool for cancer-related diagnostics, *e.g.* as an indicator of tumour aggressiveness in breast cancer (Chan et al., 2016).

Quantitative assessment of brain metabolism is another major field of application for MRS. By referring to the anatomical information from MR images (MRI) that are acquired prior to the MRS scan, the operator can control the position from which the spectroscopic information is acquired with high precision by using spectrum localization methods. MRS can thereby provide valuable information for diagnosis of, *e.g.*, epilepsy and multiple sclerosis by measuring quantities of metabolites in carefully selected areas of the brain (Stagg & Rothman, 2013). Because MRS is non-invasive and easy to perform in sensitive areas of the body, it is currently the preferred tool for quantification of metabolites in the brain.

However, in order to calculate metabolite concentrations from MRS data, individual spectra from each single metabolite that is expected to be found in the measured sample are required. Such spectra are generated separately, either by simulating them using specialized computer software, or by collecting MRS spectra from separate phantoms, each containing one of the individual metabolites. The collection of the individual spectra is then referred to as a *basis set*, and it is thus specific to the particular tissue that is being investigated, but also to the specific magnetic field strength, pulse sequence and timing parameters that are used in the study. The calculation of the metabolite concentrations is then performed using a modelling software which scales and fits the basis set components to the measured MRS data of the sample.

At present, the preclinical 7T MR system at the University of Gothenburg (GU) is used in several studies, such as studies on tumour metabolism in relation to response to treatment and effects on the normal mouse brain after exposure to incidental irradiation from cancer radiotherapy. A computer software for simulation of basis sets was recently developed at GU (Jalnefjord et al., 2018), and validated in a master thesis for a clinical MR system using the modelling software LCModel (Pettersson, 2017). However, a standardized method for calculation of metabolite concentrations from preclinical MRS data is not available. Such methods are specifically created for a particular MR vendor and for predetermined MRS protocol parameters, and the previously developed software therefore requires adaption and validation for use on the preclinical 7T MR system.

2 Aim

The general purpose of this project was to develop, validate and apply a method for non-invasive quantification of metabolites from *in vivo* MRS at the preclinical facility at GU. Specifically, to 1) adapt a method based on simulations and LCModel analysis for the point resolved spectroscopy (PRESS) sequence used at the preclinical MR system, 2) validate the method performance by measurements on a phantom with known metabolic composition, and 3) evaluate the method in the preclinical setting by determination of the metabolic composition in the healthy rodent brain and in solid tumours of a mouse model of human cancer.

3 Theoretical background

Magnetic resonance spectroscopy (MRS) is a non-invasive method that can be used to measure concentrations of metabolites within a defined volume inside the body. The following sub-sections will explain the principles of MRS and how it can provide metabolic information.

3.1 Physics of MRS

When a magnetic field is applied across an object, such as a body, it will interact with the magnetic moment of, *e.g.*, hydrogen (^{1}H) nuclei (often referred to as spin), within the object, and cause them to precess around the direction of the magnetic field. The frequency of this precession is called the Larmor frequency, f_L, and it will vary depending on the strength of the magnetic field, B_0, and the gyromagnetic ratio, γ, according to the Larmor equation (1).

$$f_L = \frac{\gamma}{2\pi} B_0 \tag{1}$$

The magnetic moment of a hydrogen nucleus can exist in quantum states either parallel or anti-parallel to the direction of the applied magnetic field. Because the parallel state is of lower energy it is favoured over the anti-parallel state and as a result there is a net magnetisation in the direction of the magnetic field. This net magnetisation is the origin of the MRS signal, which is picked up by receiver coils.

Using transmit coils, it is possible to transmit radio frequent (RF) electromagnetic waves through the object. If the frequency of the RF waves, f_{RF}, coincides with the Larmor frequency of the protons, the system will be excited, *i.e.* the net magnetisation, M, will be rotated away from the applied magnetic field. The rotation angle, α, is dependent on the RF pulse duration, t, and the strength of the magnetic component of the RF pulse, B_1, according to equation (2). An illustration of the excitation can be seen in Figure 1.

$$\alpha = \gamma B_1 t \tag{2}$$

As the RF pulse is switched off, *M* will, once again, only experience the magnetic field in the B_0-direction, and start to precess around it. The component of *M* that is perpendicular to B_0 will induce a current in the receiver coil, which is acquired as a signal, the so-called free induction decay (FID), by the receiver system. Because the nuclei of a molecule, such as a metabolite, can have varying Larmor frequencies (further explained in section 3.2), the FID will contain multiple frequencies and can, after Fourier transformation into the frequency domain, be presented as a spectrum containing information on the amplitudes of the various Larmor frequencies found inside the sample. It is through this spectrum that the metabolic composition inside the sample can be determined.

Because each nucleus in the excited system will experience fluctuation in the applied magnetic field, the transversal component of *M* will diminish over time. This phenomenon is called transversal or T2 relaxation and the rate of the T2 relaxation varies between different molecules. As such, the individual signal strength of each molecule in a spectrum acquired from an MRS measurement will vary depending on the time between the excitation of the system and acquisition of the signal, the so-called echo time (TE).

Since the gyromagnetic ratio is nuclei-specific it is necessary to decide which nucleus or isotope to build the pulse sequence parameters around. The most common isotope used for MRS is ^{1}H because of its high natural abundance and relative sensitivity. However, other isotopes do also see use, such as ^{13}C which is used for studying neuroenergetics in the brain (Stagg & Rothman, 2013).

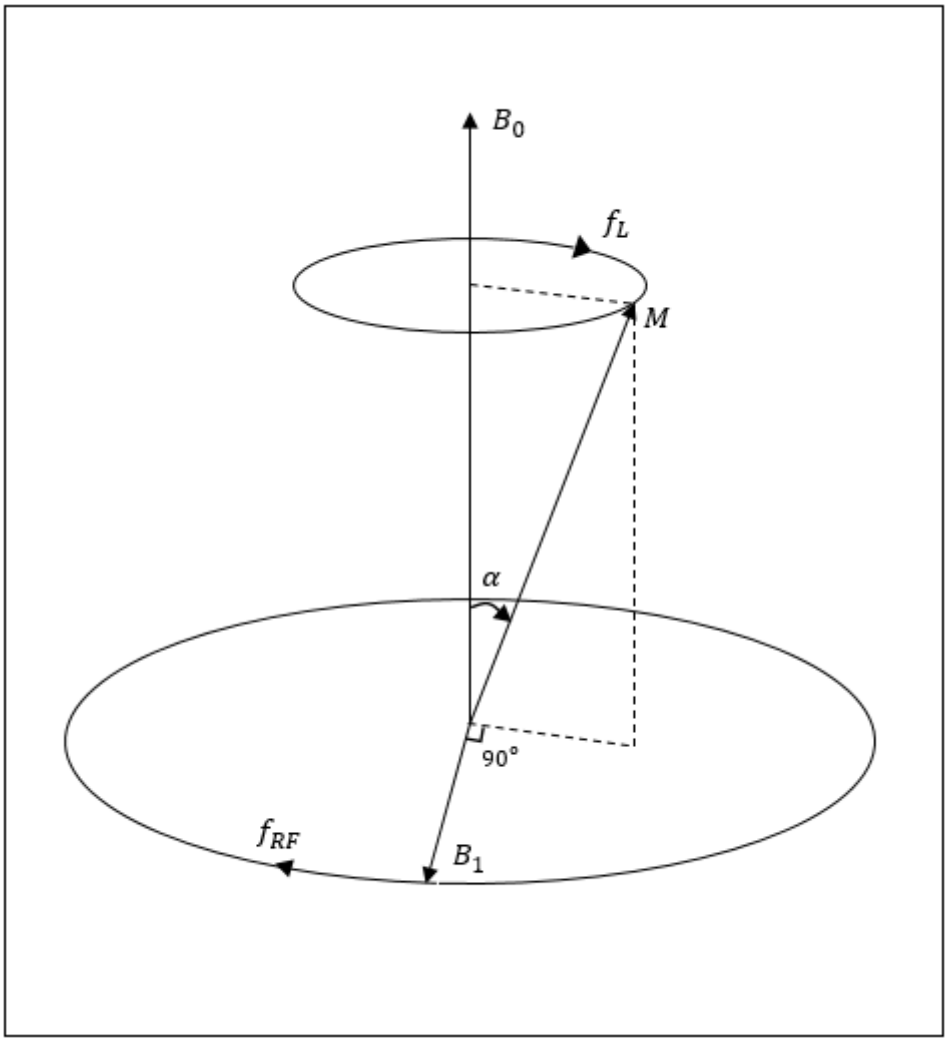

Figure 1: The net magnetic moment, *M*, will precess around the external magnetic field, B_0, at the Larmor frequency, f_L. When a radio frequent (RF) electromagnetic wave with a frequency, f_{RF}, equal to f_L enters the system during a time *t*, *M* will rotate perpendicular to the magnetic field of the RF wave, B_1, with an angle, α

3.2 Chemical shift and J-coupling

The nuclei that provide the signals used in MRS are almost exclusively part of molecule structures; in one of the simplest cases, the two hydrogen nuclei in water. Depending on the chemical structure of the molecule, electrons will be attracted to certain parts of the molecule which leads to variations in electron distribution. When a magnetic field is applied over an electron cloud, a current is induced which in turn creates small local magnetic fields. The local magnetic fields either shield against or enhance the strong external magnetic field. Nuclei on different locations in the molecule structure will thus experience slightly different net magnetic fields, and thereby precess at slightly different frequencies. The shift in Larmor frequency mediated by the electron cloud is called the chemical shift. Because the chemical shifts are specific for each molecule, they will lead to a unique spectrum for each molecule.

The Larmor frequency shifts will differ depending on the strength of the external magnetic field of the MR system. It is therefore common to state the relative chemical shift against some reference frequency. The chemical shift is then given by:

$$\delta = \frac{f_{samp} - f_{ref}}{f_{ref}} \cdot 10^6 \; ppm \tag{3}$$

where δ is the chemical shift in parts per million (ppm), f_{samp} is the sampled frequency and f_{ref} is the frequency of the reference compound. Measuring the chemical shift in this way makes it independent of the strength of the external magnetic field, which facilitates comparison of spectra obtained at different field strengths.

In addition to chemical shifts, the spectrum of a certain metabolite may also contain patterns caused by indirect dipole-dipole coupling, also called J-coupling. The J-coupling can be explained as indirect interactions between the spins mediated via the local electrons. The effect of the J-couplings is independent of the external magnetic field and can be observed as a splitting of peaks in the spectrum, typically of about 1-15 Hz for ^{1}H. An illustration of the effects of chemical shift and J-coupling on a spectrum can be seen in Figure 2.

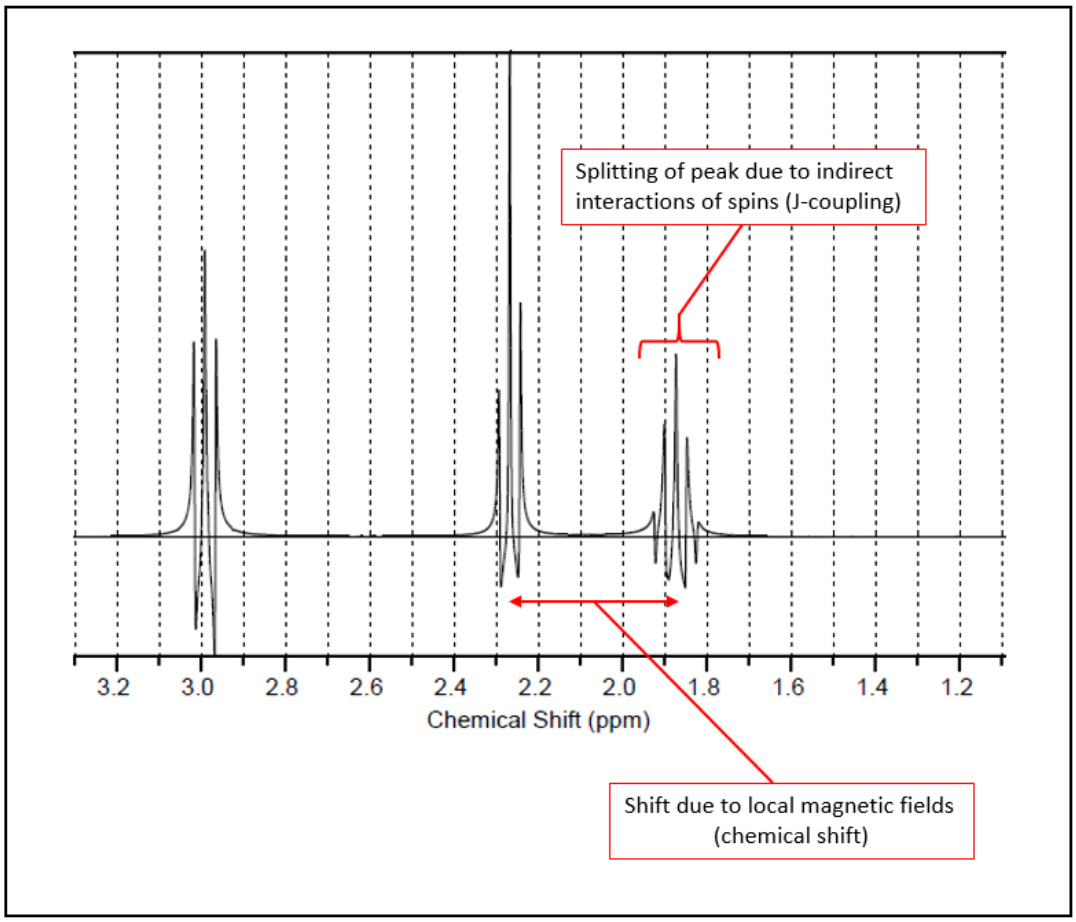

Figure 2: Due to local magnetic fields, the nuclei within a metabolite (here showing γ-aminobutyric acid) will resonate at different Larmor frequencies and thus give rise to shifts in the spectrum. Because of the indirect interactions of spins (J-coupling), the peaks in the spectrum can also appear split

3.3 Basis set and modelling

A *basis set* is a set of spectra of different, single metabolites that will, due to chemical shifts and J-couplings, possess their own unique spectral patterns. The pattern does, however, also depend on signal acquisition parameters, such as TE and magnetic field strength. When an MRS-measurement of tissue is performed, the resulting spectrum consists of a weighted sum of the spectra corresponding to all the metabolites contained within the measured sample. It is therefore possible to fit a basis set to the measured spectrum using some model fitting method, and thereby obtain information on the quantities of each detectable metabolite inside the sample. An illustration of how a basis set can be modelled to fit a measured spectrum is shown in Figure 3.

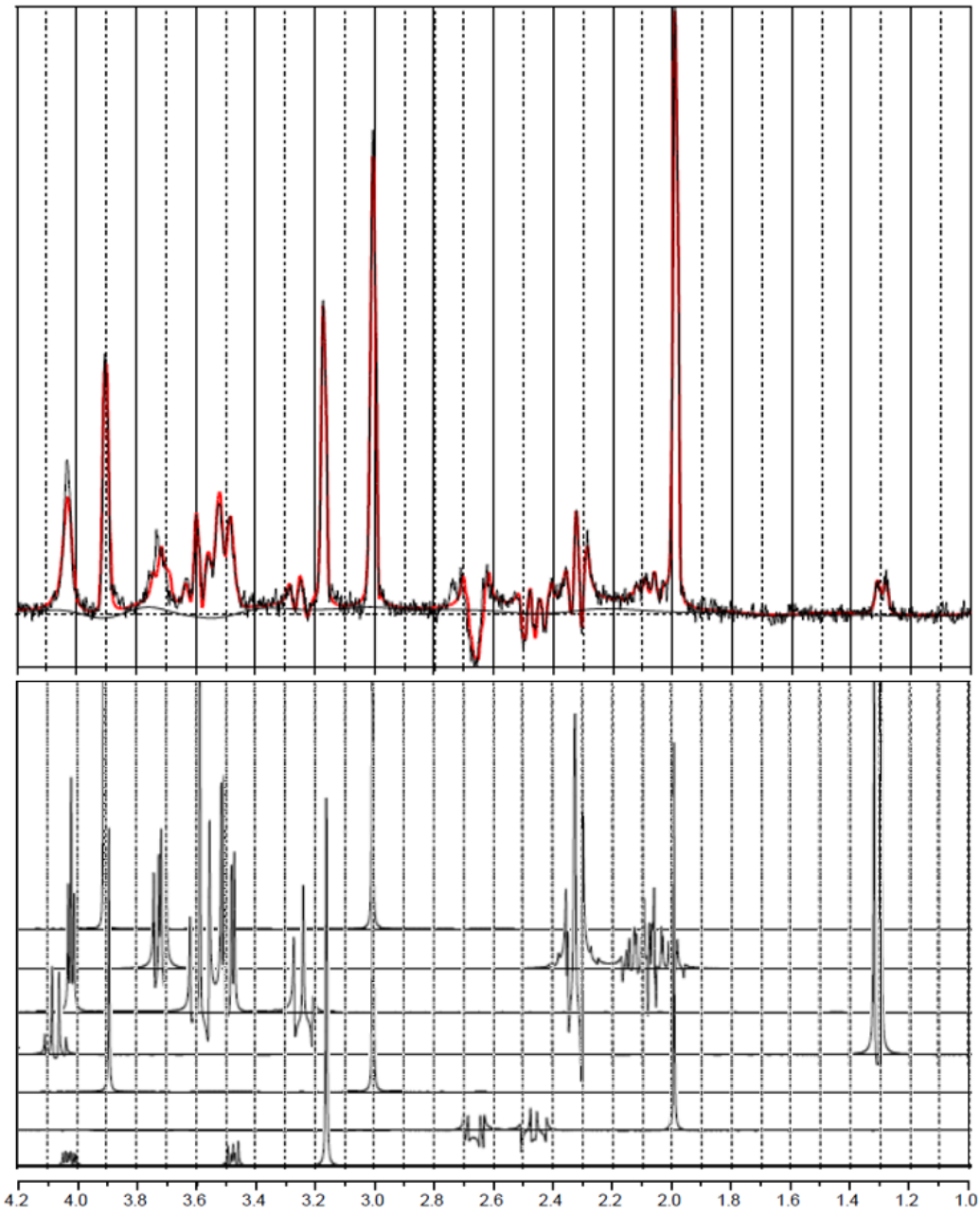

Figure 3: A basis set containing the simulated spectra of, in order from top to bottom, phosphocreatine, glutamate, myo-Inositol, lactate, creatine, N-acetylaspartate and choline (lower part in grey). The basis set is in this example fitted (upper part in red) to a measured spectrum of a phantom containing the aforementioned metabolites (upper part in black)

There are two methods to construct the basis set required for a particular study: 1) performing individual MRS measurements on each of the metabolites expected to be found and 2) simulating the included spectra by quantum mechanical calculation of the time evolution of a spin system under the influence of an MR pulse sequence. Until recent days, simulation of basis sets was difficult due to limitations in computing power. But with the technology available

today, simulation is usually preferred over measurements due to price concerns and time consumption.

When simulating a basis set, it is important to perform the simulations under the same physical conditions as the planned MRS measurement. Otherwise the spectra of the basis set will not represent the corresponding true spectra, and the model will not fit well to the data. What metabolites to include in the basis set must be guessed based on prior knowledge of the metabolic content inside the measured sample. A basis set with too many metabolites can lead to "over-fitting", meaning that the modelling algorithm finds metabolites that do not actually exist in the sample. A basis set with too few metabolites, on the other hand, can cause the modelling algorithm to overestimate the quantities of some metabolites or fail to perform a fit all together.

3.4 The MRS pulse sequence

The timing and characteristics of the gradient fields and RF pulses used for generating the MR signal in MRS determine the character of the spectrum. This is usually referred to as the pulse sequence. A pulse sequence commonly used in MRS is the point resolved spectroscopy, or PRESS, sequence. The PRESS sequence is a single-voxel sequence, meaning it aims to collect the signal from a specified volume inside the subject, *e.g.*, from a particular region within the brain. This is achieved by performing a 90°-excitation of a slice in one spatial direction followed by two 180°-excitations of slices in the remaining two spatial directions. Only the volume which has been affected by all three excitations will be phased properly and provide a signal to the receiver coils at the time of acquisition. The position and width of the slices are selected by applying a magnetic field that increases in strength linearly across the object, a so-called gradient field. This will cause the Larmor frequency of the protons to also vary linearly across the object in the same direction as the applied gradient field. By transmitting RF pulses through the object with a certain frequency bandwidth, only the protons with a Larmor frequency within the bandwidth of the RF pulse will be excited. This allows excitation of a specific volume of interest (VOI). To assure that no spins outside the VOI contribute to the measured MR signal, it is common to use so called crusher gradients to cause these spins to phase out heavily.

As described earlier, TE is the time between the 90°-excitation, *i.e.* the RF pulse that excites the spin system, and the acquisition of the signal. TE is an important parameter in MRS because it has an effect on which metabolites will be visible in the spectrum since the T2 relaxation rate varies between different metabolites. A sequence with the ability to achieve short TE will result in spectra where the majority of metabolites are still visible. On the other hand, a long TE may be desirable to remove the signals from unwanted metabolites with fast T2-relaxation rates. The main alternative sequence to PRESS in MRS is the stimulated echo acquisition mode (STEAM) sequence. Due to how the MRS signal is achieved, STEAM could, for a long time, reach far lower TEs compared with PRESS, at the price of a lower signal strength. With today's technology, however, it is possible to reach short TEs (<35 ms) with the PRESS sequence as well, making it the often-preferred choice for use in MRS (Stagg & Rothman, 2013). An illustration of the PRESS sequence can be seen in Figure 4.

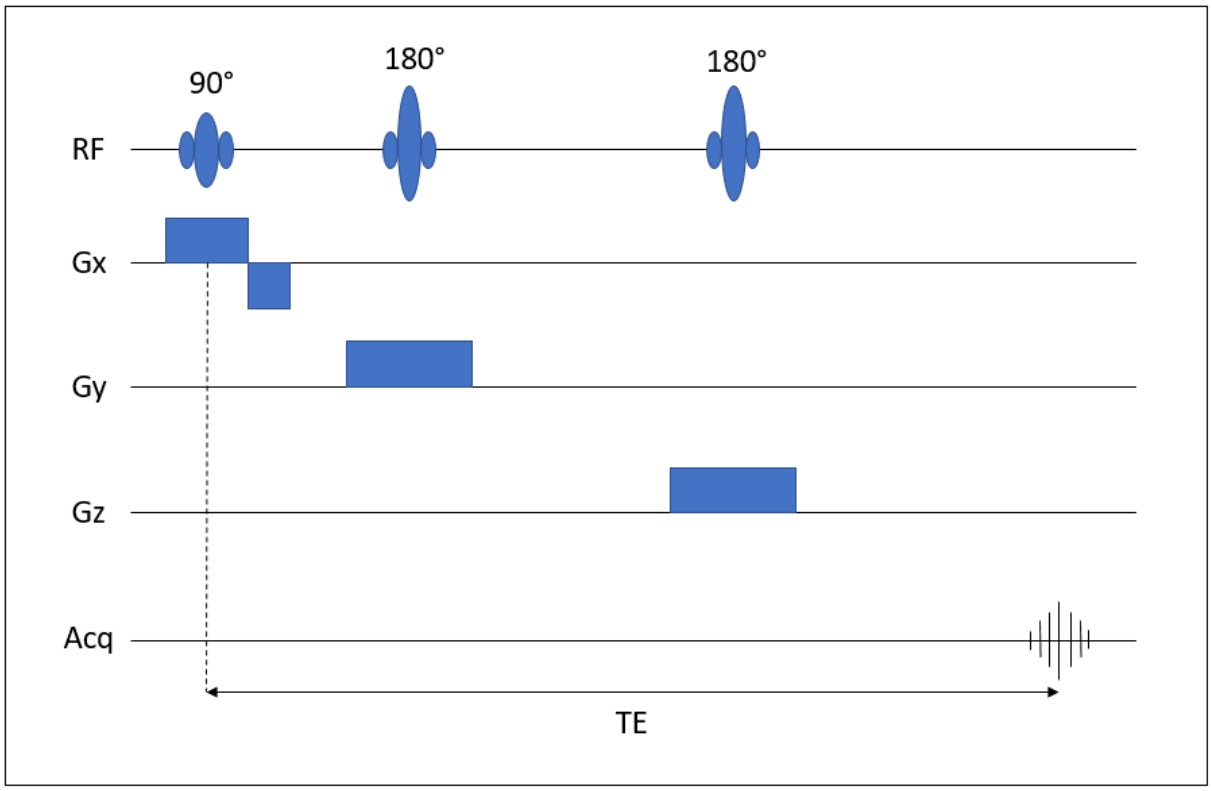

Figure 4: A diagram showing the timing of the point resolved spectroscopy (PRESS) sequence. RF represents the timing of the radio frequent pulses, with numbers indicating the flip angles that are imposed on the net magnetisation. Gx-z represent the slice selective gradients used to locally excite magnetization in the three spatial dimensions, respectively, and Acq indicates when the MRS signal is acquired by the spectrometer. Time is represented by the x-axis

4 Materials and method

4.1 MR equipment

Measurements were performed on a preclinical, horizontal-bore, 7T MR system (Bruker BioSpin MRI GmbH, Germany; software: ParaVision 5.1) equipped with water cooled gradients (maximum gradient strength 400 mT/m). A 72-mm volume coil and an actively decoupled 4-channel array rat brain coil (RAPID Biomedical Gmbh, Rimpar, Germany) were used for signal transmit and receive, respectively.

4.2 Simulations

All basis sets used for modelling were simulated using an in-house built MATLAB (MathWorks, Natick, USA) software (Jalnefjord et al., 2018) based on a recently developed simulation technique (Zhang et al., 2017). The software was originally developed for a clinical 3T MR system (Philips Achieva, The Netherlands, software release: 5.1.7.) with fundamentally different parameter definitions and validated in a previous master thesis project (Pettersson, 2017). In this work, a modified version of this software was used, which had been adapted for use on the preclinical 7T MR system. The adaption included importation of pulse sequence parameters and minor adjustments to the gradient propagator definitions. Experienced based user instructions of the software and information on which parameters are required for simulation can be found in Appendix A.

To avoid loss of signal due to chemical shift related spatial displacement, a simulated field of view (FOV) of 7×7×7 mm^3 (~175-200 % of the measured VOI-size) was used. As an example, a shift of 1 ppm from the centre frequency at 2.95 ppm corresponds to a spatial shift of 0.5 mm or less with the parameters used in this project. To achieve high-quality simulated spectra a spatial distance between sampling points of 0.175 mm was used in all simulations. The amount of sampling points used in the FID was 16 384 and the acquisition time used was 2 s. Values for chemical shifts and coupling constants were based on previous works (Govind et al., 2015; Govindaraju et al., 2000). Since these values were obtained at 37 °C they had to be temperature adjusted for the phantom measurements that were performed at 25 °C. The temperature adjustment method is described elsewhere (Wermter et al., 2017). All simulations were based on pulse sequence parameters, including RF-pulses, gradients and timings used, directly imported from files generated by ParaVision after each measurement.

4.3 Phantom validation

4.3.1 Phantom

To evaluate the accuracy of the simulations, measurements were performed on a cylindrical plastic phantom containing a mixture of metabolites of known concentrations (Table 1). In addition to the metabolites, the mixture also contained sodium hydroxide and potassium dihydrogen phosphate for pH buffering, sodium azide to prevent algae, and filtered water.

Table 1: Concentrations of metabolites in the phantom solution used for validation of the simulation code

Metabolite	Concentration (mM)
Creatine + Phosphocreatine	10
Choline	2
Glutamate	12.5
Myo-Inositol	7.5
NAA	12.5
Lactate	5

4.3.2 Experiment

Multiple phantom scans were performed using the PRESS sequence with repetition time (TR): 2500 ms and TE: 35, 72, 108 and 144 ms with corresponding number of signal averages (NSA): 512, 1024, 1024 and 2048 respectively. The number of complex data points in the FID was 2048. An offset frequency of -510.49 Hz was used. The VOI size was 3.5×3.5×3.5 mm^3 and was positioned in a region of high signal intensity, based on the image intensity in multiple reference images (Bruker triPilot) acquired in all three orthogonal directions. Automatic shimming was performed to improve the homogeneity of the static magnetic field within the VOI. A full width at half maximum (FWHM) of less than 30 Hz, based on a PRESS waterline acquisition covering the VOI, was regarded adequate for the MRS experiment.

4.3.3 Post-processing

The measured spectra were linearly modelled using simulated basis sets of corresponding TE to acquire relative concentrations to the reference metabolites choline + phosphocholine. The modelling was performed using the software LCModel and included the metabolites shown in table 1. A Cramér-Rao lower bound (CRLB) was provided by LCModel as an estimation of the accuracy of the calculated metabolite concentrations. Only metabolites found by LCModel with a CRLB of 20 % or less were considered reliable enough to include in the results.

The relative metabolite concentrations are affected by TE due to the difference in T2 relaxation between the measured metabolites and the reference metabolites. In order to compensate for this, all relative concentrations for each metabolite were plotted as a function of TE and fitted to an exponential function. The initial value of this function was then extracted to acquire the relative concentrations at TE = 0 ms, *i.e.* without any T2 relaxation effects.

4.4 *In vivo* experiments

4.4.1 Animal models and experimental setup

The *in* vivo cancer experiments were conducted on female BALB/c nude mice with subcutaneously grown xenografts of the human small intestine neuroendocrine tumour (GOT1 (Kölby et al., 2001)), and experiments on the brain were conducted on healthy C67BL/6 mice. The mice were anaesthetized using air and isoflurane (2-3 %, Isoba vet., Schering-Plough Animal-health, Denmark) during the MR experiments, body temperature was maintained using a heating pad and a pressure sensitive pad was used to monitor breathing. Total scan time was approximately 10 min for the cancer experiment and 20 min for the brain experiment. The animals were fed with standard diet and water *ad libitum*.

The experiments of this study were approved by the regional animal ethics committee in Gothenburg.

4.4.2 Experiments

The pulse sequences, reference scans and acquisition parameters described for the phantom measurements were also used for the *in vivo* measurements with some exceptions mentioned here. The NSA was 256 for the tumour measurement and 512 for the brain measurement and a TE of 30 ms was used in all *in vivo* experiments. For the tumour measurement, the VOI size was 4×4×4 mm^3, positioned in the central tumour region (Figure 5). For the brain measurement, the VOI size was 2.95×6.3×5 mm^3, positioned in the central area of the brain without including fat around the brain (Figure 6). For the brain measurement, transversal, anatomical high-resolution images (RARE) were acquired to further aid with the positioning of the VOI. The setup can be seen in Figure 5.

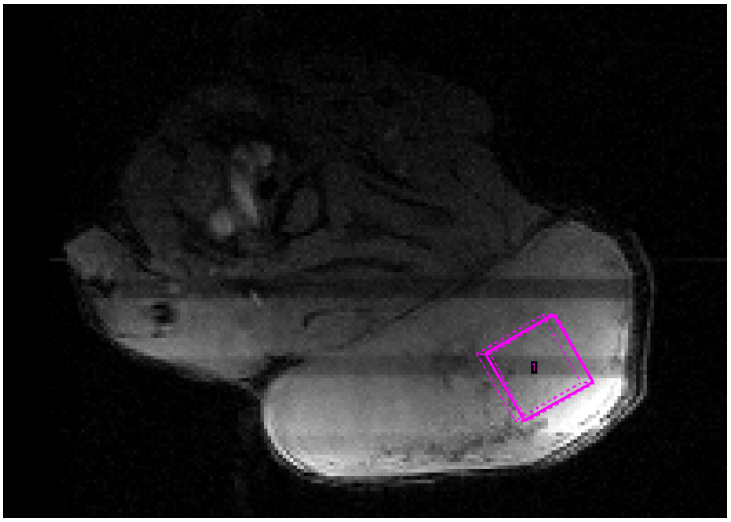

Figure 5: Geometrical positioning of the volume of interest (pink box, solid line) used in the *in vivo* MRS experiment of the human neuroendocrine tumour (hyper-intense mass in the lower part of the image) growing subcutaneously in a nude mouse (upper left half of the image). The dotted pink lines represent the VOI in other slices. The dark vertical bands appearing in the image are due to inadequate relaxation from previous scans

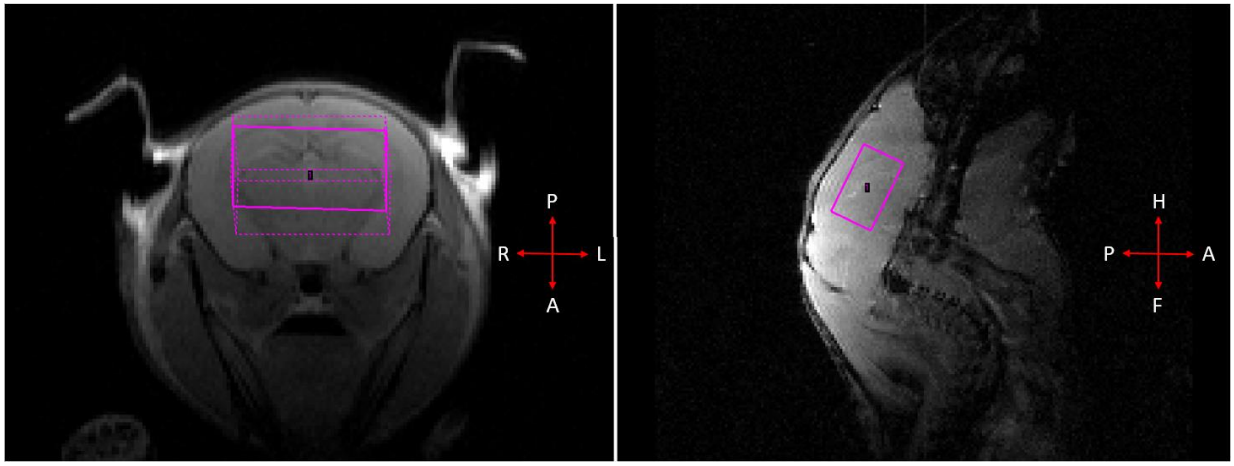

Figure 6: T1 weighted, transversal RARE image (left) of the healthy mouse brain showing the geometrical positioning of the volume of interest (pink box, solid line) used in the in vivo MRS experiment. The dotted pink lines represent the VOI in other slices. The sagittal view (right) shows the longitudinal extent of the MRS volume

4.4.3 Post-processing

Linear modelling was performed in the same way as in the phantom validation. The basis set for the tumour measurement contained the following metabolites: choline, phosphocholine, glycerophosphocholine, myo-Inositol, scyllo-Inositol, lactate, N-acetylaspartate, taurine, and glycine. Except for glycine, the basis set for the healthy brain measurement contained the same metabolites as well as creatine, phosphocreatine, aspartate, N-acetylaspartylglutamic acid, glutamine, glutamate, γ-aminobutyric acid, α-glucose, and guanine. All fits also included lipids and macromolecules from the built-in database of LCModel. The frequency ranges for the fit were [0.2, 4.2] ppm and [1.8, 4.2] ppm for the tumour and healthy brain measurements, respectively.

5 Results

5.1 Simulations

The spectra of individual metabolites generated by the simulations were in agreement with the expected appearance based on chemical shifts and J-couplings. The simulated spectrum of lactate at TE = 30 ms and 7T is shown in Figure 7 as an example of the simulation output. The chemical shifts of 4.09 and 1.31 ppm and the J-coupling split of 6.9 Hz of both peaks can be observed in the spectrum, as well as the split into four and two peaks for the peak at 4.09 and 1.31 ppm, respectively, due to multiplicity.

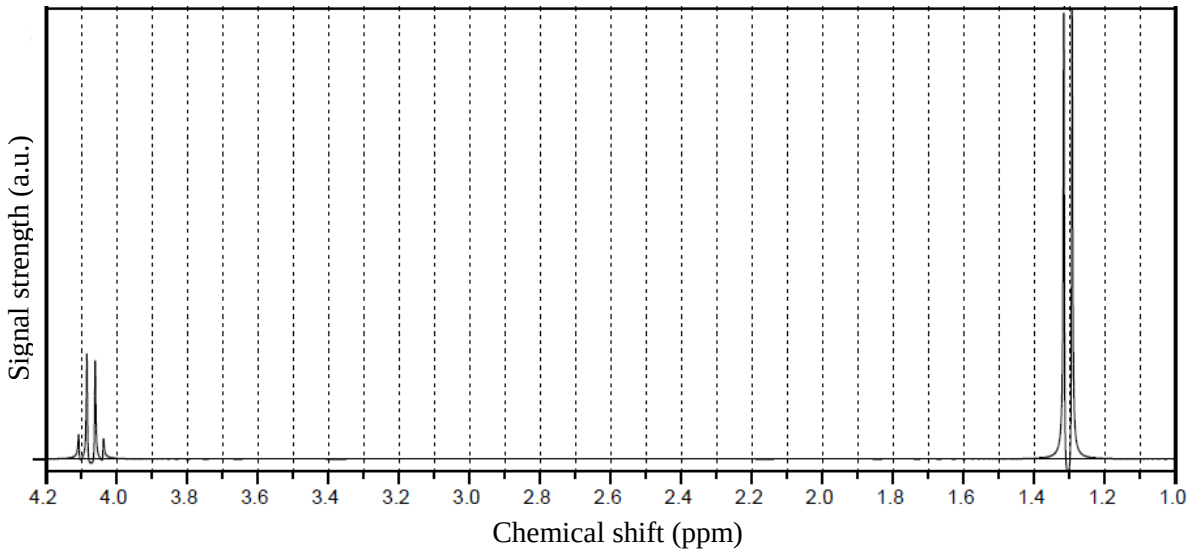

Figure 7: Simulated spectrum of the lactate metabolite at TE = 30 ms and 7T

5.2 Phantom validation

In general, the simulated basis sets were well fitted to the measured phantom data, with only minor observable residual structures that the model could not account for. The most notable remaining residual structures were observed at 2.6-2.8, 3.74 and 4.03 ppm. The residual structures at 4.03 ppm increased with increasing TE. The fit of the basis set to the spectra from the phantom measurements can be seen in Figures 8a – 8d for TE = 35, 72, 108 and 144 ms, respectively.

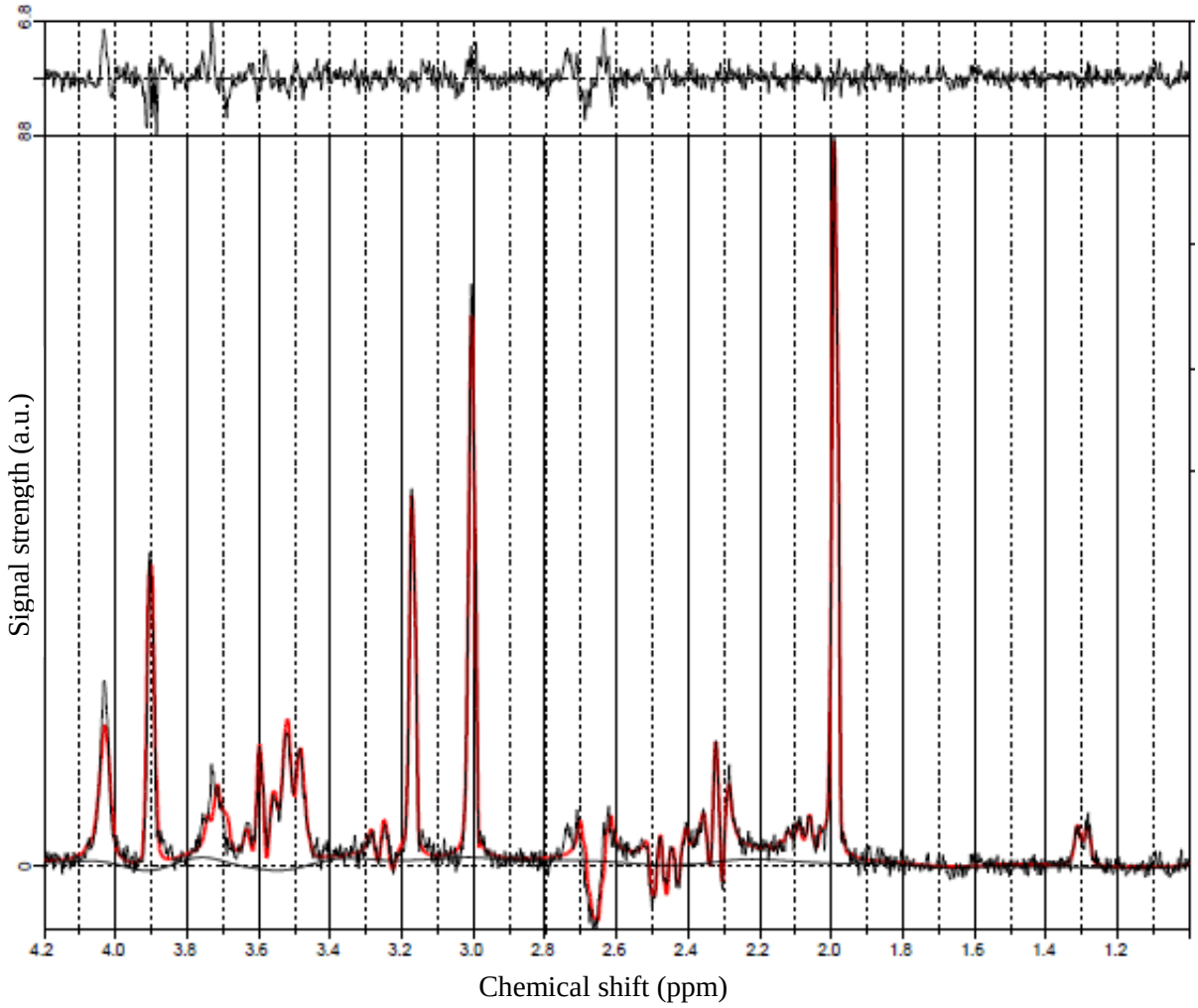

Figure 8a: The spectrum acquired from the phantom at TE = 35 ms (black) with fitted basis set superimposed (red). The base line is visible in grey beneath the spectrum. The part of the signal not accounted for by the basis set, *i.e.* the residual, is shown above the spectrum. The corresponding spectra and fitted basis sets for increasing TEs are shown in Figure 8b-8d

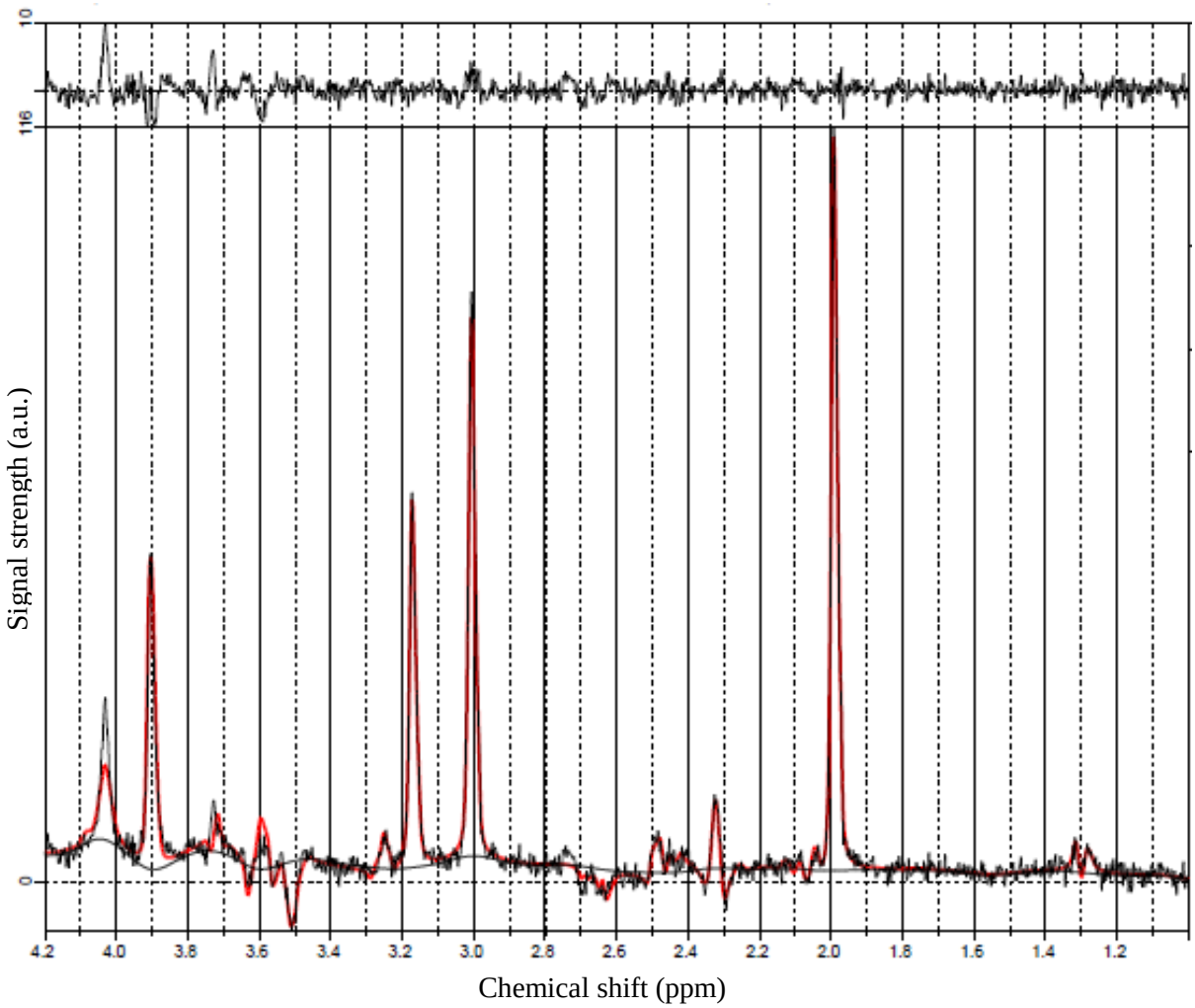

Figure 8b: The spectrum acquired from the phantom at TE = 72 ms. Note the increasing residual at 4.03 ppm

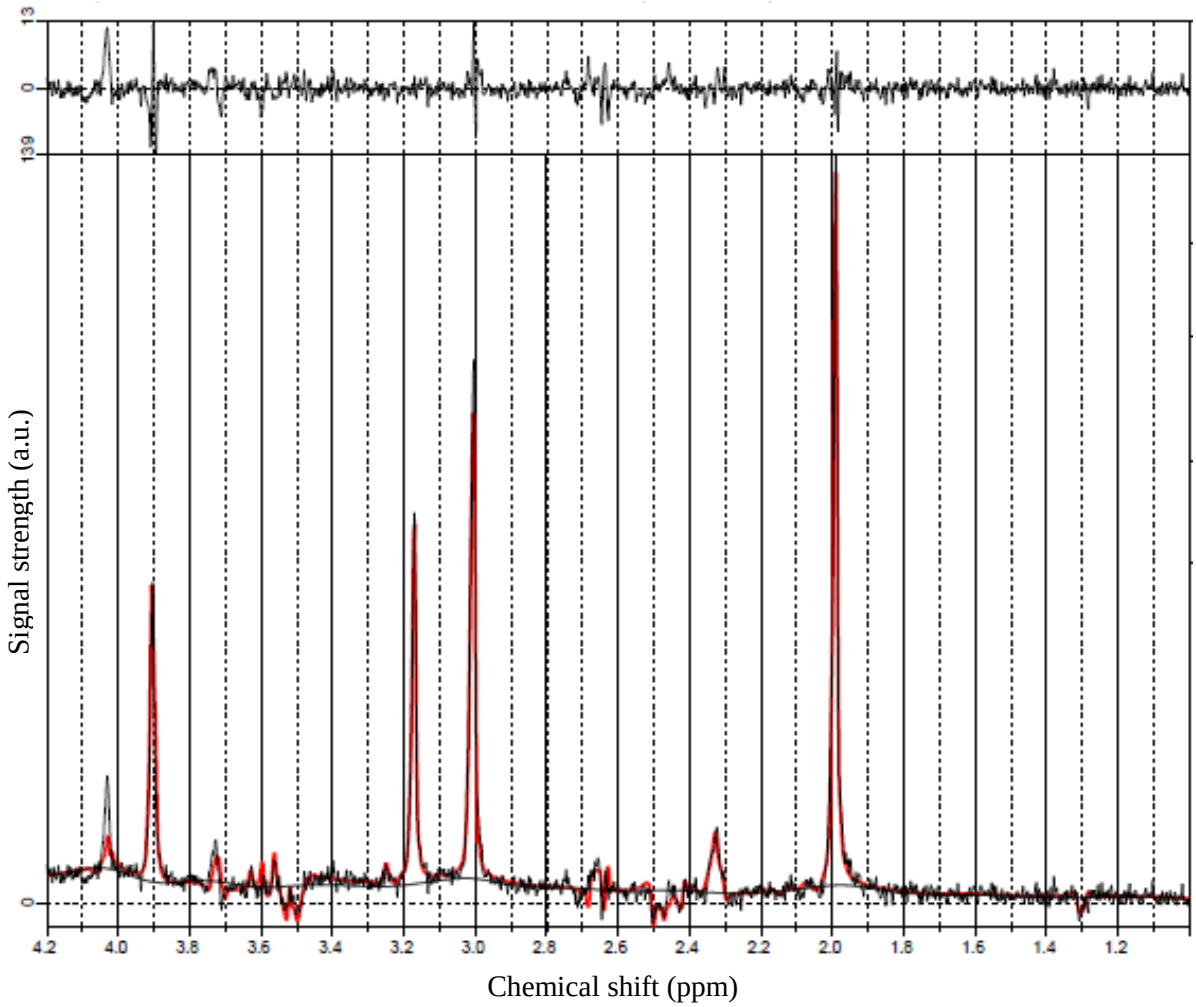

Figure 8c: The spectrum acquired from the phantom at TE = 108 ms. Note the increasing residual at 4.03 ppm

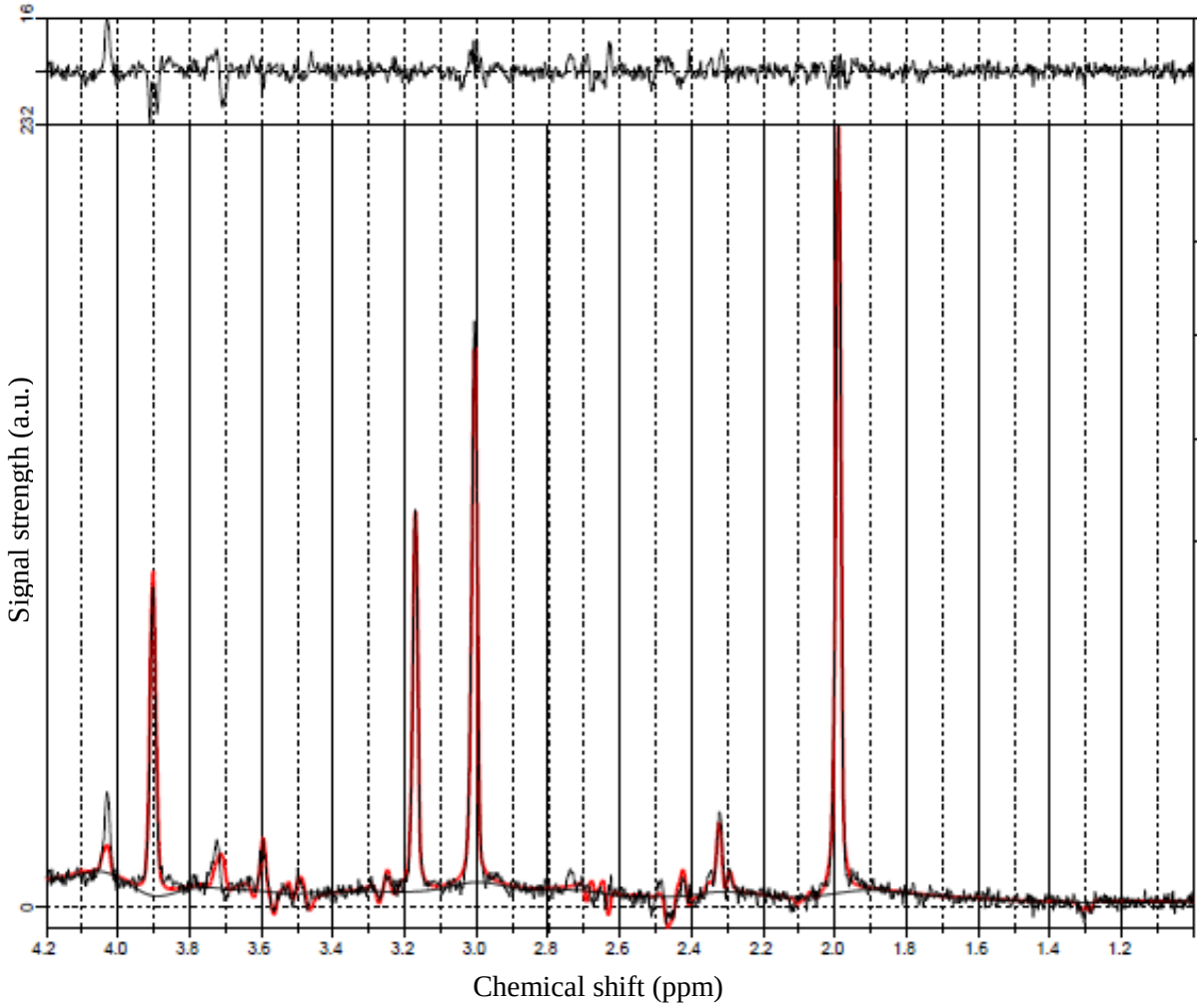

Figure 8d: The spectrum acquired from the phantom at TE = 144 ms

The measured relative concentrations to creatine + phosphocreatine for glucose, myo-Inositol, lactate, N-acetylaspartate, and choline at TE = 35, 72, 108 and 144 ms, as well as the exponential fit to the data points, are shown in Figure 9.

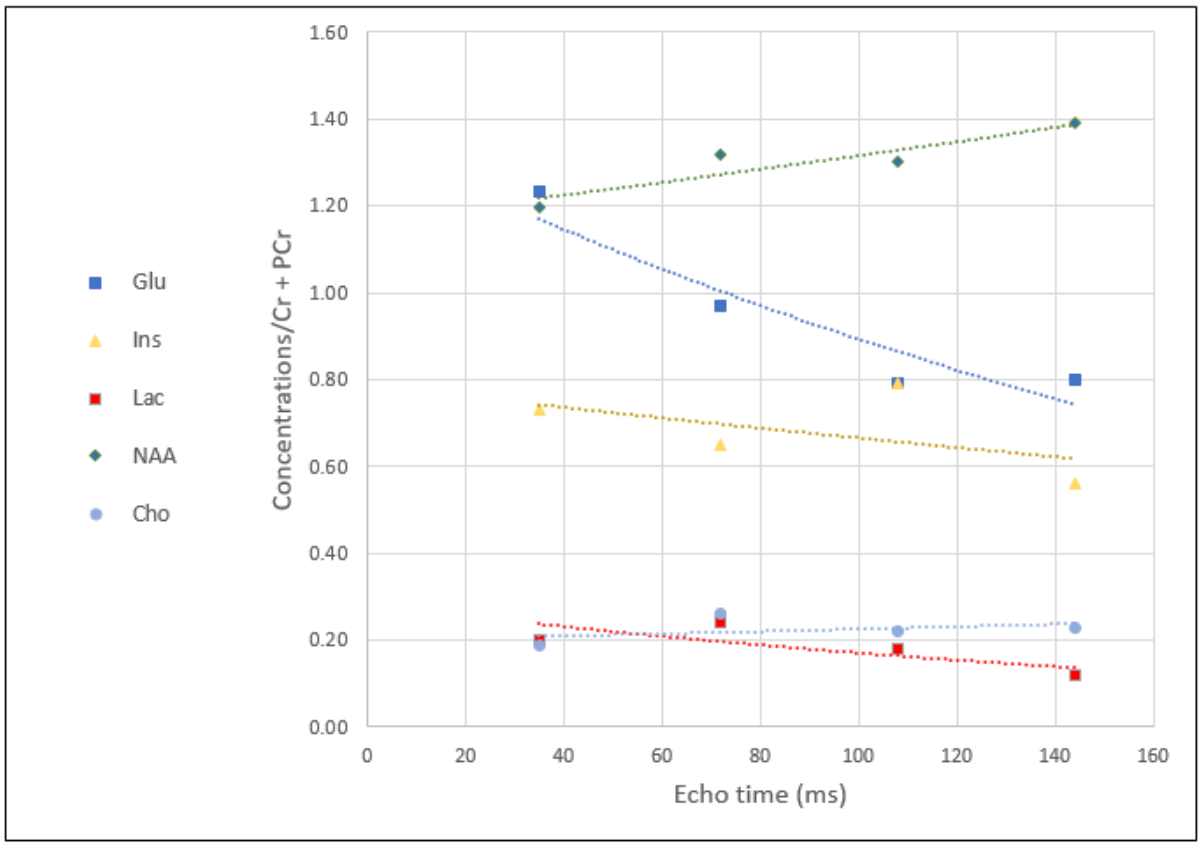

Figure 9: Measured concentrations relative to creatine + phosphocreatine for glucose (Glu), myo-Inositol (Ins), lactate (Lac), N-acetylaspartate (NAA), and choline (Cho) based on fits of basis sets to phantom measurements at TE = 35, 72, 108 and 144 ms in LCModel. The dotted lines show the exponential fit to the data points. The concentration ratio of glutamate and myo-Inositol coincide at TE = 108 ms

The difference between the calculated relative concentrations to creatine + phosphocreatine, with T2 relaxation effects compensated for, and the corresponding relative concentrations listed for the phantom solution (Table 2) were small in general. The exception was lactate where the calculated relative concentration divided by the listed relative concentration was 0.56. When calculating the relative concentration using only the measurements for TE = 72, 108 and 144 ms, however, lactate received a calculated relative concentration of 0.49 which corresponds to a ratio between the calculated and listed relative concentrations of 0.98.

Table 2: Calculated relative concentrations to creatine + phosphocreatine for glucose (Glu), myo-Inositol (Ins), lactate (Lac), N-acetylaspartate (NAA), and choline (Cho) with T2 relaxation compensated for based on the exponential fits to the data points shown in Figure 9. The listed relative concentrations for the phantom are also shown. The ratio is the calculated relative concentration divided by the listed relative concentration

Metabolite	Calculated	Listed	Ratio
Glu	1.35	1.25	1.08
Ins	0.79	0.75	1.05
Lac	0.28	0.5	0.56
NAA	1.17	1.25	0.94
Cho	0.20	0.20	1

5.3 *In vivo* experiments

The fit of the basis set to the *in vivo* tumour data was good, with little or no visible residual structures (Figure 10). The metabolites found by the modelling with a CRLB of 20 % or less were choline, phosphocholine, myo-Inositol, lactate, N-acetylaspartate, taurine and glycine. In addition to this, the combined concentration totCho (choline + phosphocholine + glycerophosphocholine) was also found with a CRLB of 20 % or less.

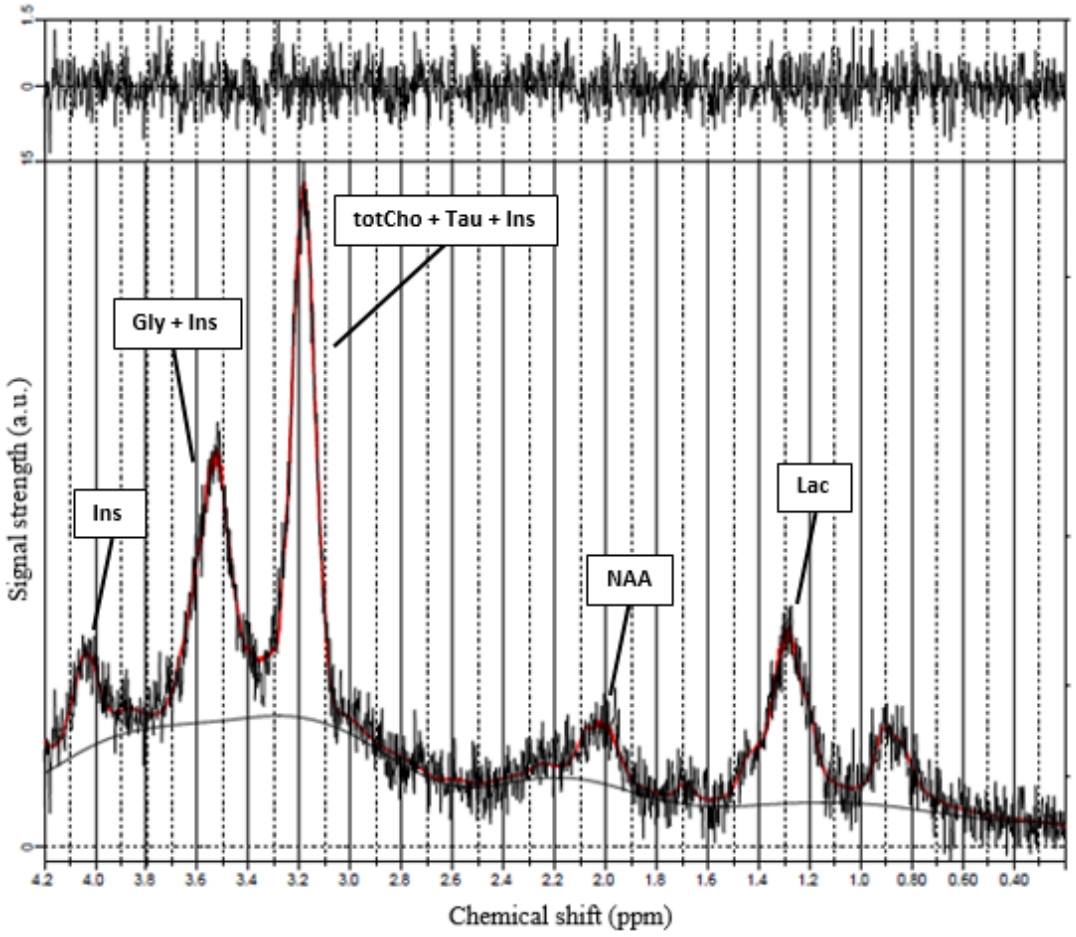

Figure 10: The spectrum acquired from the in vivo measurement on a subcutaneous tumour in a mouse model of a human neuroendocrine tumour at TE = 30 ms (black) with fitted basis set superimposed (red). The base line is visible in grey beneath the spectrum. The part of the signal not accounted for by the basis set, *i.e.* the residual, is shown above the spectrum. The metabolite contributions to the most significant peaks in the spectrum are shown for myo-Inositol (Ins), glycine (Gly), choline + phosphocholine + glycerophosphocholine (totCho), taurine (Tau), N-acetylaspartate (NAA) and lactate (Lac)

The fit of the basis set to the measured *in* vivo brain data was good in general, with few residual structures (Figure 11). The fit with the base line included can be seen in Appendix B. The individual metabolites found by the modelling with a CRLB of 20 % or less were glutamate, phosphocreatine, myo-Inositol, N-acetylaspartate, N-acetylaspartylglutamate, taurine, phosphocholine and glycine. In addition to this, the combined concentrations totCho (choline + phosphocholine + glycerophosphocholine), totCr (creatine + phosphocreatine) and Glx (glutamate + glutamine) were also found with a CRLB of 20 % or less.

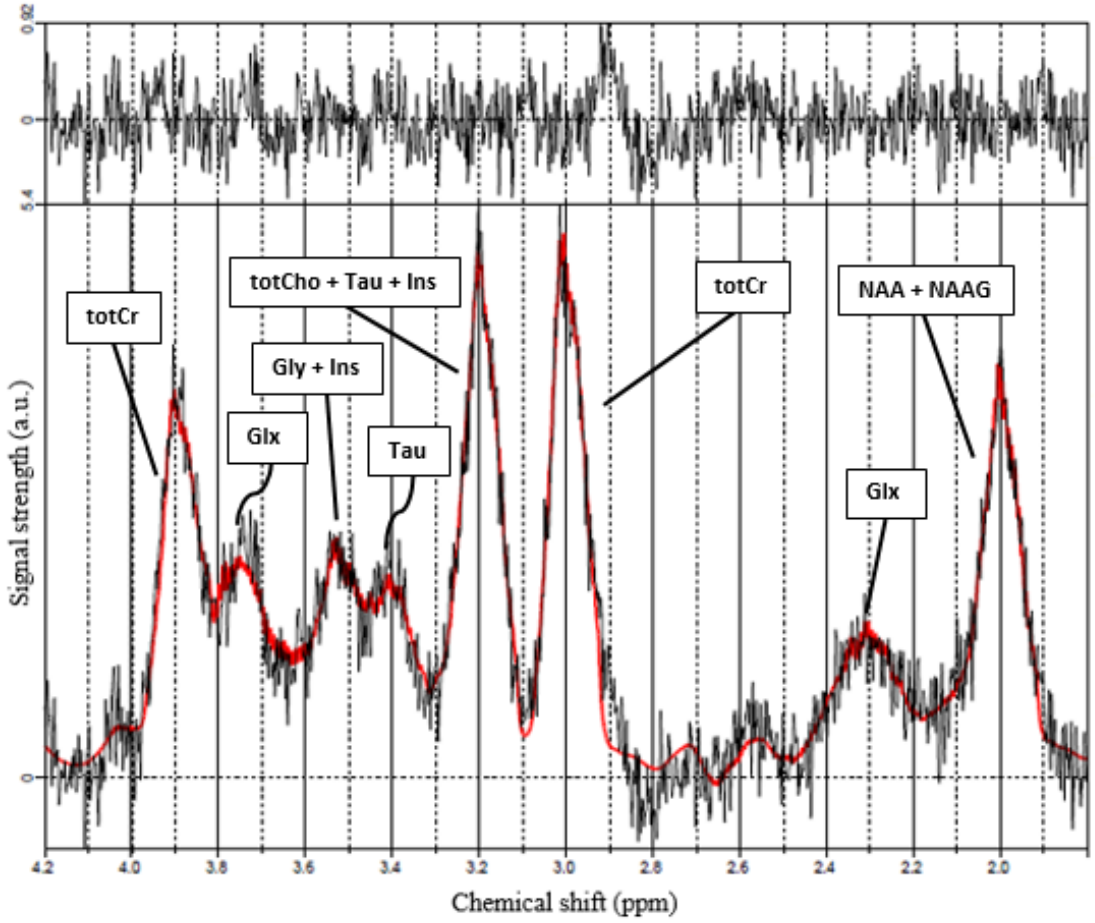

Figure 11: The spectrum acquired from the *in vivo* measurement on a healthy mouse brain at TE = 30 ms (black) with fitted basis set superimposed (red) and the baseline subtracted. The part of the signal not accounted for by the basis set, *i.e.* the residual, is shown above the spectrum. The modelling was performed from 1.8 ppm to avoid miss-fits due to the large contribution of fat present at lower ppm. The metabolite contributions to the most significant peaks in the spectrum are shown for creatine + phosphocreatine (totCr), glutamate + glutamine (Glx), glycine (Gly), myo-Inositol (Ins), choline + phosphocholine + glycerophosphocholine (totCho), N-acetylaspartate (NAA) and N-acetylaspartylglutamate (NAAG). The spectrum with the baseline included can be seen in Appendix B

6 Discussion

In this project, a method for non-invasive quantification of metabolites from *in vivo* MRS at the preclinical facility at the University of Gothenburg was developed and validated. The method was based on a previously developed software for simulation of basis sets for determination of metabolite concentrations from MRS measurements, but was designed for use on a 3T clinical system with vendor specific parameter file structure. The software had to be adapted for use on the preclinical 7T MR system which required reprogramming of a MATLAB-based code to read the required parameters from the preclinical system, as well as validation experiments, including phantom measurements and *in vivo* measurements on a mouse model of human cancer and the healthy mouse brain.

In general, the validation of the simulation software showed few residual structures in the fit of the phantom data which implies that the simulated spectra were of good quality.

There were, however, a few recurring residual structures that could be observed for all TE, most notably at chemical shifts at 4.03 ppm. A possible explanation is the fact that the phantom solution available to us was outdated by 2 years (labelled with a durability of 1 year). The chemical structure of some of the metabolites may have changed over time with possible effects on the chemical shifts and J-couplings. Since metabolic alterations were not accounted for in the simulation, they may have caused the residual structures observed in the spectrum evaluations.

System imperfections may also cause spectrum artefacts and lead to residual structures. A comparison with a measurement on the same phantom solution performed on the clinical 3T MR system, and evaluated using the same simulation software revealed highly similar residual structures, which indicates that the 7T system did not cause the residual structures. The simulation software has also been validated in a previous master thesis using the clinical 3T MR system and a recently put together phantom solution, which did not show the residual structures apparent in the validation performed in this work. This makes it unlikely that the residual structures appeared due to programmatic errors in the simulation code.

Spatial displacement of the VOI due to chemical shift is a common concern when performing MRS. If the VOI is placed too close to the border of the tissue structure of interest, there is a possibility that the VOI will end up outside the volume for metabolites with a significant shift from the reference frequency. This can lead to differences in the relative signal strength between peaks of the same metabolite at different frequencies and thus give rise to residual structures. In this work, spatial displacement due to chemical shift was accounted for by calculating the maximum possible displacement and restricting the VOI position accordingly, and VOI displacement should therefore not have caused the residual structures observed.

It should be noted that the residual structures discussed above were small, and probably with little or no effects on *in vivo* evaluation of metabolite concentrations where physiological noise and magnetic field distortions are probably of greater concern.

The relative concentrations calculated in the phantom validation showed very good results in general, with small deviations from the listed relative concentrations of the phantom solution. The exception was lactate which showed a ratio between the calculated and listed relative concentrations of 0.56. Interestingly, when excluding the first measurement of TE = 35 ms, this

ratio was improved to 0.98, which indicates that the large deviation may be related to issues with the first scan.

In the phantom measurements for validation, a TR of 2500 ms was used which could have caused saturation effects due to inadequate longitudinal relaxation between successive scans. If relaxation rates differed between the metabolites it could have affected the calculated phantom concentrations. The longitudinal relaxation rate of a metabolite is dependent on its immediate environment. However, based on T1 relaxation rates acquired for metabolites in the brain in previous works, the expected error in the relative concentrations for the validation performed in this work due to differences in T1 relaxation between metabolites would be approximatively 15 % or less (Xin et al., 2013). In future phantom measurements it is suggested to use a higher TR to reduce the effects of T1 relaxation.

The ability to study metabolites non-invasively and longitudinally in tumours is of high interest for clinical and preclinical research. For example, lactate, taurine, choline and glycine have shown elevated concentrations in colorectal cancer compared with normal tissue, and concentrations have been correlated with tumour aggressiveness in breast cancer (Chan et al., 2009; Chan et al., 2016). Furthermore, lower pre-treatment concentrations of glycine in locally advanced rectal cancer has been correlated with increased progression free survival after neoadjuvant chemotherapy (Redalen et al., 2016). The method used in this work for determining metabolites *in vivo* in tumours showed good results, and lactate, taurine, choline and glycine were all detected by LCModel with a CRLB of less than 20 %, indicating that the levels of these metabolites were accurately determined by the method validated in this work.

When performing the measurements on the healthy mouse brain, small VOIs were first attempted to cover specific anatomical parts of the brain, such as the cortex or the hippocampus. When attempting this, however, the signal to noise ratio (SNR) was too poor to accurately perform a fit to the spectrum. To improve the SNR, a larger VOI was chosen to cover a significant part of the brain. However, measurements with the larger VOI caused a significant peak to appear in the range [0, 1.8] ppm. This was likely caused by acquisition of fat signals from outside the VOI due to the previously mentioned spatial displacement. The appearance of this peak made fitting of the basis set difficult in the lower ppm range and the fit was therefore performed in the range [1.8, 4.2] ppm instead. Unfortunately, this meant that lactate and alanine, two metabolites commonly found in the brain, could not be fitted by LCModel as their most significant peaks are present below 1.8 ppm. LCModel was, however, able to accurately (CRLB < 20 %) detect Glx (glutamate + glutamine), totCr (creatine + phosphocreatine), myo-Inositol, NAA, NAAG, taurine, totCho (choline + phosphocholine + glycerophosphocholine) and glycine, all of which have been found in the healthy mouse brain in previous studies (Duarte et al., 2014; Kulak et al., 2010; Rana et al., 2013).

A significant baseline was observed in the *in vivo* measurements. The baseline is estimated by LCModel to compensate for the contributions of macromolecules (MM) and lipids and it is important to be aware of the shape of the baseline since it may have an effect on the quality of the fit. In the *in vivo* modelling, the baseline was expected to be significant due to the presence of MMs and lipids. To simplify the estimation of the baseline done by LCModel, a metabolite-nulled spectrum, containing only spectral patterns from MM and lipids, can be measured and subtracted for each *in vivo* spectrum. Although this will reduce the SNR, there will be fewer corrections left to compensate for by LCModel. Subtraction of metabolite-nulled spectrums

was not performed in this work, but may potentially be used to improve the results in future studies.

Future improvements of the method could include expanding the method for absolute quantification of metabolite concentrations, this however requires knowledge of the water concentration in the VOI which is difficult to measure non-invasively. The simulation software could be further developed to include additional pulse sequences which may be of interest when performing *in vivo* MRS, such as the STEAM sequence. T2-relaxation effects could also be included in the simulation software to provide more accurate metabolite concentrations at higher TE.

7 Conclusion

In this work, a method for preclinical *in vivo*, non-invasive metabolite quantification based on MRS experiments was developed and validated. The method was based on a previous master thesis project and was developed for a clinical MR system. It therefore required programmatic adjustments in order to export correct data from the preclinical system, as well as thorough validation by phantom measurements. The method will provide a necessary means for evaluation of both current and future MRS studies at the preclinical MR facility at the University of Gothenburg, with immediate application on, *e.g.*, ongoing studies on cancer therapies.

Parameters describing the pulse sequence could be extracted successfully from the preclinical MR system and thus enabled creation of basis sets through simulations. The validation of the method performance revealed basis sets well fitted to the spectra, as well as accurately determined metabolite concentrations. The *in vivo* experiments on the mouse model of human cancer and on the healthy mouse brain both showed well fitted basis sets. The cancer measurement resulted in metabolite profiles typical of cancer and the brain measurement resulted in metabolic profiles which were in agreement with previous MRS studies on healthy mouse brains.

8 Reference list

Bokacheva, L., Ackerstaff, E., LeKaye, H. C., Zakian, K., & Koutcher, J. A. (2014). High-field small animal magnetic resonance oncology studies. *Phys Med Biol, 59*(2), R65-R127.

Chan, E. C., Koh, P. K., Mal, M., Cheah, P. Y., Eu, K. W., Backshall, A., . . . Keun, H. C. (2009). Metabolic profiling of human colorectal cancer using high-resolution magic angle spinning nuclear magnetic resonance (HR-MAS NMR) spectroscopy and gas chromatography mass spectrometry (GC/MS). *J Proteome Res, 8*(1), 352-361.

Chan, K. W., Jiang, L., Cheng, M., Wijnen, J. P., Liu, G., Huang, P., . . . Glunde, K. (2016). CEST-MRI detects metabolite levels altered by breast cancer cell aggressiveness and chemotherapy response. *NMR Biomed, 29*(6), 806-816. doi:10.1002/nbm.3526

Duarte, J. M., Do, K. Q., & Gruetter, R. (2014). Longitudinal neurochemical modifications in the aging mouse brain measured in vivo by 1H magnetic resonance spectroscopy. *Neurobiol Aging, 35*(7), 1660-1668.

Gonzalez Hernando, C., Esteban, L., Canas, T., Van den Brule, E., & Pastrana, M. (2010). The role of magnetic resonance imaging in oncology. *Clin Transl Oncol, 12*(9), 606-613.

Govind, V., Young, K., & Maudsley, A. A. (2015). Corrigendum: proton NMR chemical shifts and coupling constants for brain metabolites. Govindaraju V, Young K, Maudsley AA, NMR Biomed. 2000; 13: 129-153. *NMR Biomed, 28*(7), 923-924.

Govindaraju, V., Young, K., & Maudsley, A. A. (2000). Proton NMR chemical shifts and coupling constants for brain metabolites. *NMR Biomed, 13*(3), 129-153.

Jalnefjord, O., Pettersson, P., & Ljungberg, M. (2018). *Improved Absolute Metabolite Quantification by Localized Magnetic Resonance Spectroscopy Simulations*. European congress of medical physics. Copenhagen.

Kulak, A., Duarte, J. M., Do, K. Q., & Gruetter, R. (2010). Neurochemical profile of the developing mouse cortex determined by in vivo 1H NMR spectroscopy at 14.1 T and the effect of recurrent anaesthesia. *J Neurochem, 115*(6), 1466-1477.

Kölby, L., Bernhardt, P., Ahlman, H., Wangberg, B., Johanson, V., Wigander, A., . . . Nilsson, O. (2001). A transplantable human carcinoid as model for somatostatin receptor-mediated and amine transporter-mediated radionuclide uptake. *Am J Pathol, 158*(2), 745-755.

Pettersson, P. (2017). *Simulation of MR spectroscopy basis sets for quantitative analysis with LCModel.* University of Gothenburg, Göteborg. Retrieved from https://radfys.gu.se/utbildning/Rapporter_fr_n_examensarbeten

Rana, P., Khan, A. R., Modi, S., Hemanth Kumar, B. S., Javed, S., Tripathi, R. P., & Khushu, S. (2013). Altered brain metabolism after whole body irradiation in mice: a preliminary in vivo 1H MRS study. *Int J Radiat Biol, 89*(3), 212-218.

Redalen, K. R., Sitter, B., Bathen, T. F., Groholt, K. K., Hole, K. H., Dueland, S., . . . Seierstad, T. (2016). High tumor glycine concentration is an adverse prognostic factor in locally advanced rectal cancer. *Radiother Oncol, 118*(2), 393-398.

Sand, O., & Toverud, K. C. (2007). *Människokroppen : fysiologi och anatomi* (2. uppl. [översättning: Inger Bolinder-Palmér ...] ed.). Stockholm: Stockholm : Liber.

Stagg, C., & Rothman, D. L. (2013). *Magnetic resonance spectroscopy tools for neuroscience research and emerging clinical applications*. Amsterdam: Amsterdam : Academic Press.

Wermter, F. C., Mitschke, N., Bock, C., & Dreher, W. (2017). Temperature dependence of (1)H NMR chemical shifts and its influence on estimated metabolite concentrations. *Magma, 30*(6), 579-590.

Xin, L., Schaller, B., Mlynarik, V., Lu, H., & Gruetter, R. (2013). Proton T1 relaxation times of metabolites in human occipital white and gray matter at 7 T. *Magn Reson Med, 69*(4), 931-936.

Zhang, Y., An, L., & Shen, J. (2017). Fast computation of full density matrix of multispin systems for spatially localized in vivo magnetic resonance spectroscopy. *Med Phys, 44*(8), 4169-4178.

Appendix A – The simulation code

A.1 Experienced based user instructions

To perform the simulations, the code requires a multitude of parameters, these are explained in section A.2. It is also necessary to define names, chemical shifts, and coupling constants of all metabolites to be simulated. The simulation itself is based on the principles of quantum mechanics and creating density operators that describe the average quantum states of the system at a given time. A more detailed explanation on how the quantum physics approach has been implemented into the simulation code is explained in (Jalnefjord et al., 2018). Once the simulation of the chosen metabolites is completed, a RAW-file containing their FID will be generated for each metabolite, as this is the file format accepted by the LCModel software. The RAW-files can then be imported and used to create a basis set in LCModel. The reference metabolite used for calculation of chemical shift in LCModel is 4,4-dimethyl-4-silapentane-1-sulfonic acid, or DSS, and a spectrum for this metabolite is therefore generated at the start of every simulation. A pseudocode explaining the general sequence of the simulation code can be seen in Figure (12).

```
Define simulation parameters

Define pulse sequence parameters

Simulate a reference peak for DSS

For (metabolites to be simulated)

        Simulate metabolite

        Generate RAW-file

End
```

Figure 12: Pseudocode for the general sequence of the simulation code used for creation of basis sets

A.2 Parameters

Two different types of parameters are required by the code for the simulation to function: *simulation parameters* and *pulse sequence parameters*. The *simulation parameters* are changed directly by the user in the code and should be modified before every simulation. The *pulse sequence parameters* are extracted automatically from specific files generated by ParaVision.

A.2.1 Simulation parameters

The following is a list of simulation parameters that require user input before every simulation:

- B_0 *field strength*
- *Spectrometer frequency*
- *Simulated FOV*
- *Resolution*
- *Sampling points*
- *Acquisition time*
- *Metabolites to be simulated*

Special caution should be taken when choosing the simulated FOV as this must be appropriately large so that there is no signal lost. The simulated FOV must therefore always be at least as large as the VOI used in the measurement and, due to the spatial displacement from the chemical shifts, most likely significantly larger. Do also note that increasing the resolution will increase the amount of spatial points simulated and therefore also the simulation time. Because the simulation uses a one-dimensional approach (Zhang et al., 2017), the simulation time scales linearly with the resolution. In other words, if the resolution is doubled in each direction so too will the simulation time be doubled.

A.2.2 Pulse sequence parameters

The files required by the code to import necessary pulse sequence parameters from the Bruker system are automatically generated by ParaVision after each measurement. The exception to this is the *preemphasis file* which can be found locally in the ParaVision directory. The following is a list of the files required as well as the parameters imported from them:

- pulseprogram
  - *Indexes for gradient strengths*
  - *Indexes for pulse times and pulse shapes*
  - *Phase cycling scheme*
- acqp
  - *Gradient trim values*
  - *Delays*
- method
  - *Gradient calibration constant*
  - *Pulse durations*
- spnamN, N = 1,2,3, …
  - *Pulse shape of pulse N*
- Preemphasis file
  - *Ramp time*

The *pulseprogram* file contains information, or indexes, about the timings, pulses and gradients to be used in the pulse sequence. The actual values for these indexes are then acquired from the *acqp* and *method* files. The values for the gradient strengths however, are not acquired directly but are instead calculated using the *gradient calibration constant* and *gradient trim values*. It could also be of interest to know that the *ramp time* parameter is not the true ramp time used in the pulse sequence. Rather, it is the time it would take for an ideal ramp to reach the plateau of the gradient with the same dephasing as the true ramp. Therefore, this parameter is not dependant on the ramp mode chosen by the user in ParaVision.

Appendix B

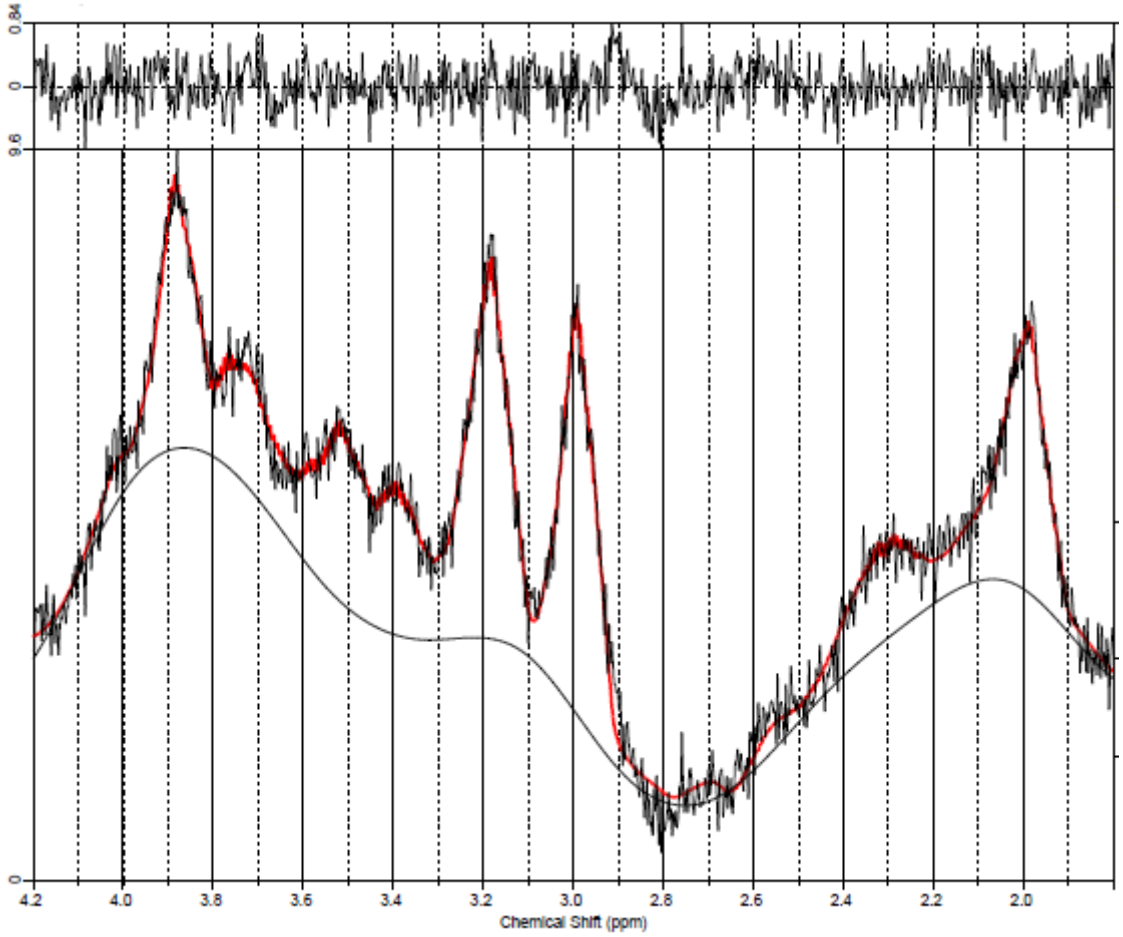

Figure 11: The spectrum acquired from the measurement of a healthy mouse brain using TE = 30 ms (black) with fitted basis set superimposed (red). The base line is visible in grey beneath the spectrum. The part of the signal not accounted for by the basis set, *i.e.* the residual, is shown above the spectrum. The modelling was performed from 1.8 ppm to avoid miss-fits due to the large contribution of fat present at lower ppm